European Journal of Pharmaceutics and Biopharmaceutics 75 (2010) 26–32

Contents lists available at ScienceDirect

European Journal of Pharmaceutics and Biopharmaceutics

journal homepage: www.elsevier.com/locate/ejpb

Research paper

A comparative study of chitosan and chitosan/cyclodextrin nanoparticles as potential carriers for the oral delivery of small peptides ☆

Adriana Trapani [a], Angela Lopedota [a], Massimo Franco [a], Nicola Cioffi [b], Eliana Ieva [b], Marcos Garcia-Fuentes [c], Maria José Alonso [c,*]

[a] Dept. of Pharmaceutical Chemistry, Bari University, Aldo Moro, Bari, Italy
[b] Dept. of Chemistry, Bari University, Bari, Italy
[c] Dept. of Pharmaceutical Technology, Santiago de Compostela University, Santiago de Compostela, Spain

ARTICLE INFO

Article history:
Received 26 June 2009
15 December 2009
Accepted in revised form 20 January 2010
Available online 25 January 2010

Keywords:
Glutathione
Chitosan
Cyclodextrins
Nanoparticles
Oral administration

ABSTRACT

The aim of this study was to characterize new nanoparticles (NPs) containing chitosan (CS), or CS/cyclodextrin (CDs), and evaluate their potential for the oral delivery of the peptide glutathione (GSH). More precisely, NP formulations composed of CS, CS/α-CD and CS/sulphobutyl ether-β-cyclodextrin (SBE_{7m}-β-CD) were investigated for this application. CS/CD NPs showed particle sizes ranging from 200 to 500 nm. GSH was loaded more efficiently in CS/SBE_{7m}-β-CD NPs by forming a complex between the tripeptide and the CD. X-ray Photoelectron Spectroscopy (XPS) analysis suggested that GSH is located in the core of CS/SBE_{7m}-β-CD NPs and that it is almost absent from the NP surface. Release studies performed *in vitro* at pH 1.2 and pH 6.8 showed that NP release properties can be modulated by selecting an appropriate CD. Transport studies performed in the frog intestine model confirmed that both CS and CS/CD nanoparticles could induce permeabilization of the intestinal epithelia. However, CS/SBE_{7m}-β-CD NPs provided absorption-enhancing properties in all segments of the duodenum, whereas CS NPs effect was restricted to the first segment of the duodenum. From the data obtained, we believe that CS/CD nanoparticles might represent an interesting technological platform for the oral administration of small peptides.

1. Introduction

Glutathione (γ-glutamylcysteinylglycine, GSH) is the major thiolated small peptide in mammalian cells. Its reducing and nucleophilic properties render GSH a fundamental redox buffer that prevents the oxidative damage caused by free radicals from oxygen species circulating in the body. GSH is also speculated to influence gene expression in two ways: (i) via its reactive oxidant species (ROS) scavenging role and (ii) via protein glutathionylation [1]. The clinical value of this small peptide includes its use for the treatment of alcohol and drug poisoning, as well as for protection against cytotoxic chemotherapy and radiation trauma [2]. Currently, GSH is only available on the market as parenteral dosage forms (Gluthion®) because of its low and variable oral bioavailability [3]. This limited absorption has been mainly attributed to the chemical and enzymatic degradation of the peptide in the jejunum. More specifically, it is known that the thiol group of the cysteine moiety in GSH is susceptible to enzymatic (γ-glutamyltranspeptidase) and non-enzymatic pH-dependent oxidation [4], leading to the formation of inactive products. However, the oral route continues to be the most desirable pathway for drug administration, particularly for therapeutic agents in which several doses are necessary.

To achieve oral delivery of GSH, drug carrier systems are required to protect this drug from the gastrointestinal environment and from enzymatic degradation. Several nanoparticle (NP) prototypes from biodegradable polymers have been proposed for transmucosal drug delivery [5–7]. Among them, NPs based on the polysaccharide chitosan (CS) have shown particularly promising results due to their intrinsic properties including biocompatibility, mucoadhesion and ability to transiently open the tight junctions of the intestinal barrier [8–10]. CS NPs have already shown capacity to deliver orally hydrophilic macromolecules as confirmed both in cellular models and in animal experiments [11]. Recently, we reported the formation of a new NP carrier based on the combination of CS and CDs [12,13]. Originally, the inclusion of CDs in the NP structures was designed as a modification intended to improve

☆ This work is dedicated to the memory of Prof. Gaetano Liso, recently deceased, for his example of man and scientist.

* Corresponding author. Department of Pharmacy and Pharmaceutical Technology, Faculty of Pharmacy, University of Santiago de Compostela, 15782 Santiago de Compostela, Spain. Tel.: +34 981 594 488; fax: +34 981 547 148.
E-mail address: mariaj.alonso@usc.es (M.J. Alonso).

0939-6411/$ - see front matter © 2010 Elsevier B.V. All rights reserved.
doi:10.1016/j.ejpb.2010.01.010

the capacity of these carriers to load poorly soluble drug [14]. However, it has became evident that these NPs can also load hydrophilic molecules with high efficiency [13] and enhance their transport across mucosal surfaces [15,16]. In the case of GSH, this possibility is even more attractive, as previous studies performed by us have confirmed the possible inclusion of this molecule inside the cavity of CDs and that this interaction prevents the degradation of this molecule by endopeptidases [17].

In summary, taking into account the increasing clinical value of GSH, we have investigated the potential of CS and CS/CD NPs as potential carrier systems for the oral delivery of this small peptide. The resulting prototypes were extensively characterized with regard to their physicochemical properties, their capacity to load and release GSH and the capacity to protect and promote the transport of GSH across the intestinal frog sac model.

2. Materials and methods

2.1. Materials

The following chemicals were obtained from commercial sources and used as received. Chitosan hydrochloride (UP CL 113, Mw = 110 kDa, deacetylation degree = 86% according to manufacturer instructions) was purchased from Pronova Biopolymer (Norway). Alpha-cyclodextrin (α-CD, Mw = 972 Da) was kindly given by Wacker-Chemie (Peschiera Borromeo, Italy). Glutathione (GSH), glycerol (over 99.5% purity) and Pentasodium tripolyphospate (TPP) were purchased from Sigma–Aldrich (Milan, Italy). Sulphobutyl ether-β-cyclodextrin sodium salt (SBE_{7m}-β-CD, Mw = 2163 Da, average substitution degree = 6.40) was bought by CyDex, Inc. (USA). Both CDs were kept in a desiccator until to be used. Ultrapure water (Carlo Erba, Italy) was used throughout the study. All other chemicals were reagent grade or better.

Frog Ringer (FR) solution (pH = 6.0) was prepared as follows: NaH_2PO_4 H_2O 5.0 mmol, K_2HPO_4 1.0 mmol, $CaCl_2$ $2H_2O$ 1.0 mmol and the amount of NaCl required to reach 230 ± 10 mOsm/kg (Micro-Osmometer Automatic Type 13 RS, Hermann Roebling Messtechnik, Berlin, Germany).

2.2. Nanoparticle preparation

CS or CS/CD-based NPs were prepared according to a modified ionic gelation method [12,18]. (a) *CS Nanoparticles:* 1.5 ml of a GSH aqueous solution (0.10%w/v) was mixed with 1.5 ml of a CS solution (0.40%w/v). NPs were spontaneously formed upon addition of 1 ml of TPP aqueous solution (0.15%w/v) to 3 ml of the CS/GSH solution under magnetic stirring. (b) *CS/CD NPs* were prepared differently depending on the type of CD used. However, for both α-CD and SBE_{7m}-β-CD, 1:1 M ratio stoichiometry CD:GSH complexes were previously prepared by co-incubation of the aqueous solutions of both compounds for 24 h at room temperature and under moderate stirring. For α-CD:GSH, an aqueous solution was prepared by adding 23.15 mg of α-CD and 7.0 mg of GSH to 7 ml of distilled water. For SBE_{7m}-β-CD:GSH, an aqueous solution was prepared by adding 31.5 mg of SBE_{7m}-β-CD and 4.5 mg of GSH to 7 ml of distilled water. To prepare CS/α-CD NPs, 1.5 ml of the solution containing α-CD:GSH complexes were mixed with 1.5 ml of a CS solution (0.40%w/v). The resulting solution was mixed with 1 ml of TPP aqueous solution (0.15%w/v) under magnetic stirring, leading to spontaneous NP precipitation. To prepare CS/SBE_{7m}-β-CD NPs, a 3 ml CS solution (0.20%w/v) was mixed with 1 ml of the SBE_{7m}-β-CD:GSH solution, a process already reported to lead to NP formation [19]. For all formulations, the resulting NPs were isolated by centrifugation (16,000*g*, 45 min, Eppendorf 5415D, Eppendorf, Germany) and resuspended in ultrapure water by manual shaking.

2.3. Physicochemical and morphological characterization of nanoparticles

Particle size and polydispersity index (PI) were determined in double distilled water by photon correlation spectroscopy (PCS) using a Zetasizer NanoZS (ZEN 3600, Malvern, UK). The determination of the ζ-potential was performed using laser Doppler anemometry (Zetasizer NanoZS, ZEN 3600, Malvern, UK) after dilution with KCl 1 mM.

The morphological examination of the NP prototypes was performed by transmission electron microscopy (TEM) (CM12 Philips, Eindhoven, Netherlands). For sample preparation, NPs were resuspended in water, stained with 2% (w/v) phosphotungstic acid, placed on copper grids with Formvar® films and dried overnight at room temperature.

2.4. HPLC analysis

High-performance liquid chromatography (HPLC) analyses were performed with a Waters (Waters Corp., Milford, MA) Model 600 pump equipped with a Waters 2996 photodiode array detector (set at the wavelength of 220 nm), a 20 μl loop injection autosampler (Waters 717 plus) and processed by Empower™ Software Build. For analysis, a reversed phase Synergy Hydro-RP (25 cm × 4.6 mm; 4 μm particles; Phenomenex, Torrance, CA) column in conjunction with a precolumn C18 insert was eluted with 1:99 (v:v) acetonitrile:0.025 M phosphate buffer (pH 2.7) in isocratic mode. The flow rate was maintained at 0.7 ml/min. Standard calibration curves were prepared at 220 nm wavelength using 0.025 M phosphate buffer (pH 2.7) as solvent. Calibration curve linearity ($r^2 > 0.999$) was maintained over the range of concentrations tested (5.46×10^{-6} M–3.32×10^{-3} M). The retention times of GSH and its disulphide degradation product (GSSG) were 7.2 and 18 min, respectively. Under these conditions, the quantification limit was determined to be 2 μg/ml for both GSH and GSSG.

2.4.1. Determination of GSH encapsulation efficiency

The Encapsulation Efficiency (EE) of the tripeptide to the particles was calculated by an indirect method. CS or CS/CD NPs were isolated from free GSH by centrifugation (16,000*g*, 45 min, Eppendorf 5415D, Eppendorf, Germany), and free GSH in the supernatant was quantified by HPLC as described above. Experiments were performed in triplicate and the encapsulation efficiency was calculated as follows:

$$\%EE = 100 \times (\text{total GSH} - \text{free GSH})/\text{total GSH}$$

2.4.2. Determination of SBE_{7m}-β-CD content in NPs

SBE_{7m}-β-CD was quantified in the supernatants of unloaded and GSH-loaded CS/SBE_{7m}-β-CD NPs by spectrophotometric analysis of the fading of phenolphthalein alkaline solutions [20,21]. Briefly, a 3 mM phenolphthalein stock solution in methanol was diluted 1:100 in 0.05 M carbonate buffer (pH 10.5). Freeze-dried supernatants of NPs were dissolved in 1000 μl of acetic acid (0.1%, v/v). 400 μl of this mixture were added to 2.6 ml of diluted phenolphthalein solution prepared as described above. The absorbance at 553 nm of resulting solution was measured by Perkin Elmer Lamba Bio 20 spectrophotometer. For quantification, the SBE_{7m}-β-CD content was calculated by comparing the results to that of a standard curve obtained by using standard CD solutions. Linearity was checked in the range from 0.10 mg/ml to 2.20 mg/ml.

2.5. XPS analysis

X-ray Photoelectron Spectroscopy (XPS) analysis was performed to explore the differences in chemical composition at

various depths from the NP surface. CS/SBE_{7m}-β-CD NPs loaded with GSH were analyzed with a Thermo VG Theta Probe spectrometer equipped with a micro-spot monochromatized Al Kα source. Conventional XPS analyses provided information on the elemental composition and chemical speciation of the NP outer surface (5 nm thick), while ion-etching assisted Depth Profile XPS was used to quantify the in-depth distribution of GSH in the NPs. In particular, thiol and sulphonate chemical environments (resolved at the baseline in the S_{2p} high-resolution spectra) were chosen as unambiguous labels for GSH and SBE_{7m}-β-CDs, respectively.

2.6. In vitro release study

In vitro release of GSH from loaded CS and CS/CD NPs was carried out for 3 h in simulated gastric (pH 1.2) and intestinal (pH 6.8) medium without enzymes and performed according to USP XXVI recommendations. Freshly prepared CS and CS/CD NPs were isolated in Eppendorf tubes with a 10 μl glycerol bed laid in the bottom of the tube, set to help on NP resuspension. In screw-capped test tubes, each formulation was resuspended in 0.4 ml of distilled water and the resulting resuspended formulation was mixed with 1 ml of release medium (simulated gastric or intestinal medium) and incubated at 37 °C under mechanical agitation (150 oscillations/min). At appropriate time intervals, an aliquot (0.4 ml) was withdrawn and centrifuged (16,000*g*, 40 min, Eppendorf 5415D, Eppendorf, Germany). The initial volume of release medium was maintained by refilling 0.4 ml of the same medium after each withdrawal. The supernatant was analyzed for GSH content by HPLC as described above. GSH in solution was dissolved in the same media and analyzed at the same time points, as a control for GSH degradation. Each experiment was performed in triplicate.

2.7. Transport studies in the frog intestinal sac model

Animal care and handling throughout the experimental procedure was carried out in accordance with the European Community Council Directive of 24 November 1986 (86/609/EEC). Healthy frogs of the species *Rana esculenta* (Animali da Laboratorio R. Orefice, Arzano, Italy) were housed in a cold room, in an aquarium, and without food. The aquarium was thoroughly washed once a week. The frogs were killed by decapitation and pithing of the spinal cord, and small intestines were quickly removed by laparotomy. The excised piece of intestine was immediately washed with Frog Ringer (FR) solution, at room temperature, to remove the intestinal content.

Two intestinal segments of approximately 2.50 cm in length were tied at one end with a silk suture and then used to assess the permeability of this model epithelium to GSH, both in presence or in the absence of two nanocarriers: blank CS and blank CS/SBE_{7m}-β-CD NPs. Permeability studies for all GSH formulations were performed both in the proximal and in the distal segment of duodenum. The integrity of these intestinal membrane sacs was checked throughout the study by using phloridzin as internal standard at the concentration of 160×10^{-6} M. The sacs were filled with (i) free GSH in FR solution, (ii) free GSH added to resuspended blank CS NPs, or (iii) free GSH added to blank resuspended CS/SBE_{7m}-β-CD NPs. The volume of the donor compartment was in the range 0.1–0.3 ml. The sacs were sealed and immersed in vials (2.70 cm width × 5.73 cm high) containing 1.0–2.0 ml of FR solution. These vials were incubated in a water shaking bath (Isco mod. SBH Milan, Italy), at 26 ± 0.1 °C (100 rpm) for 5 h. At fixed time points, the amount of GSH in the acceptor chamber was quantified by withdrawing a 0.2 ml sample from the vial and measuring GSH concentration by HPLC. The initial volume of the external medium was maintained by refilling the volume withdrawn with fresh FR.

The apparent permeability coefficient P_{app} (cm/s) was calculated using the following equation:

$$P_{app} = dQ/dt(1/A \times 60 \times c_0)$$

where dQ/dt is the permeability rate (mg/s), namely the amount of GSH permeating the tissue in time t (min); A is the area of exposed frog intestine tissue (around 2.5 cm^2); c_0 is the initial GSH concentration (mg/ml) inside the intestinal sac.

2.8. Statistics

Data from different experimental groups were compared by a one-way ANOVA with $p < 0.05$ (GraphPad Prism v.4.00, GraphPad Software, Inc., San Diego, CA). Tukey tests were used for post hoc contrast.

3. Results and discussion

In this work, we aimed at the design and characterization of new drug nanocarriers for the oral delivery of low molecular weight peptides. More specifically, in this work, we studied chitosan nanoparticles and chitosan/cyclodextrin NPs as potential carriers for oral delivery of GSH. The rationale behind the selection of these nanocarriers can be summarized as follows: (i) CS NPs present very good record as oral delivery systems of poorly permeable drugs [9,22]. Recently, CS/CD NPs have also shown promising results as delivery systems of hydrophilic macromolecules [15,16]. (ii) GSH has already shown the capability to interact with α-CD [17], a characteristic that might increase the affinity of this drug for the NP matrix. (iii) The formation of GSH:α-CD complexes stabilizes this molecule towards its degradation by endopeptidases [17].

In the following lines, we describe the preparation of CS and CS/CD NPs loaded with GSH, their physicochemical properties are presented, and the capability to release GSH in simulated physiological fluids and promote GSH transport across model epithelia are also reported.

3.1. Formation and characterization of CS and CS/CD NPs loaded with GSH

To exclude the possible formation of covalent linkages between CS and GSH, or the induction of degradative processes arising from co-incubating these molecules, the chemical stability of GSH in an aqueous CS solution was checked by HPLC up to 24 h at room temperature. This study allowed us to exclude any chemical modification of GSH during this incubation process (data not shown).

CS and CS/CD NPs were prepared as described in Section 2.3. In the specific case of the CS/CD NPs system, two CDs with very different properties were selected: α-CD and SBE_{7m}-β-CD. Overall, the methods for CS NP preparation were similar to those described by Calvo et al. [18] and CS/CD NPs were formed by a method similar to that previously reported [12]. However, in this work, GSH:CD complexes were formed prior to NP preparation through the co-incubation of both molecules for 24 h.

Table 1 displays the physicochemical properties of the different NPs prepared. It is well known that the size of CS NPs depends on the concentration of CS, the concentration of TPP and the CS/TPP ratio [23]. However, in this case, other factors affecting NP size were detected, namely, the nature and the amount of the CD incorporated (Table 1). Indeed, NPs incorporating the neutral α-CD were bigger than the other formulations: 512 nm average particle size and moderately wide size distribution (PI = 0.40–0.60). On the other hand, the incorporation of the negatively charged CD, SBE_{7m}-β-CD, resulted in NPs that were markedly smaller than the

Table 1
Physicochemical properties of unloaded CS, CS/α-CD and CS/SBE_{7m}-β-CD NPs and the corresponding GSH loaded particles. PI: polydispersity index; ζ: zeta potential; EE: association efficiency. Mean ± SD are reported, $n = 6$.

Formulation	Concentration GSH (%w/v)	Concentration CD (%w/v)	Size (nm)	PI	ζ (mV)	EE (%)
Unloaded CS NPs	0	0	350 ± 30	0.25–0.39	+30.5 ± 2.4	0
Unloaded CS/α-CD NPs	0	0.31	512 ± 41	0.40–0.60	+36.1 ± 0.7	0
Unloaded CS/SBE_{7m}-β-CD NPs	0	0.45	210 ± 14	0.06–0.15	+28.4 ± 1.2	0
GSH loaded CS NPs	0.1	0	350 ± 30	0.44–0.54	+30.0 ± 6.3	7.1 ± 3.0
GSH loaded CS/α-CD NPs	0.1	0.31	500 ± 50	0.45–0.57	+36.6 ± 0.9	5.6 ± 1.1
GSH loaded CS/SBE_{7m}-β-CD NPs	0.06	0.45	190 ± 20	0.19–0.32	+28.7 ± 1.5	25.1 ± 2.3

other formulations: 210 nm average particle size, very narrow particle distribution (PI = 0.06–0.15). Overall, these results confirm the capacity of neutral and anionic CDs to influence the process of CS assembly during NP formation, as it has been discussed elsewhere [12]. In all cases, positive zeta potential values were detected, suggesting that CS is mainly located on the surface of the particles. However, it is interesting to note that CS/α-CD NPs presented slightly higher zeta potential values than the other formulations. The addition of GSH did not produce significant changes to the physicochemical properties of the NPs, except for the PI of the CS and CS/SBE_{7m}-β-CD NP formulation that increased moderately (Table 1).

TEM imaging is widely used to investigate NP morphology. Regular and spherical morphology was revealed by TEM both for CS and CS/CD NPs, and this was observed irrespective of the presence or the absence of GSH (Fig. 1). CS/α-CD NPs morphology was very similar to that of CS NPs (data not shown), whereas some differences were observed with respect to CS/SBE_{7m}-β-CD NPs. More concretely, a tight structure is typically observed for CS NPs and CS/α-CD NPs, while a more loose outer shell is observed in CS/SBE_{7m}-β-CD NPs. This layer is attributed to more loosely bound CS chains. Particle size measured by TEM resulted in smaller particle size values than those measured by photon correlation spectroscopy, a typical result arising from chitosan dehydration during TEM sample preparation [24].

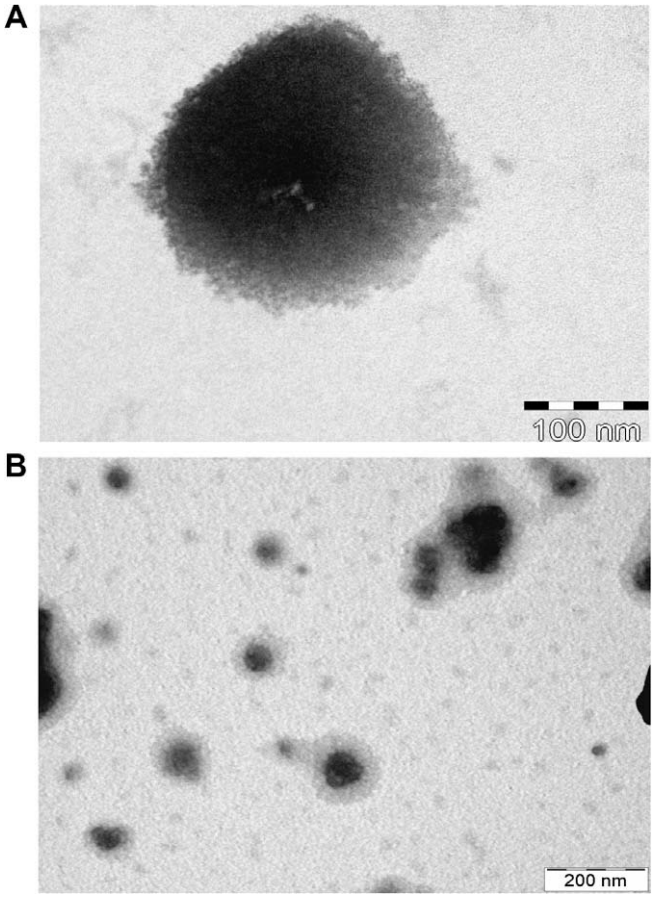

Fig. 1. TEM images of NP formulations: (A) CS NPs and (B) CS/SBE_{7m}-β-CD NPs.

The capacity of the different NP systems to load GSH was determined. Firstly, we could observe that CS and CS/α-CD NPs presented very low encapsulation efficiency (EE) (i.e. below 10%, Table 1). The low affinity of GSH to CS matrix might relate to the low Mw of the peptide and to the presence of only one net negative charge in its chemical structure. Incorporation of GSH as complex with α-CD did not result on improved EE. On the other hand, the EE increased to 25% for CS/SBE_{7m}-β-CD NPs (Table 1). This value represents a 3.5-fold increase in EE in relation to standard CS NPs. GSH encapsulation efficacy can be understood by considering the encapsulation process as a two-step procedure: (1) the association of GSH to the CD and (2) the inclusion of the CDs into the nanocarrier. GSH association to α-CD is in the range 55–70 M^{-1} at 25 °C as we have shown by NMR investigations in a previous work [17]. Although some signals overlapping prevented such precise measurement of the complexation constants, our data suggest that GSH is complexed with SBE_{7m}-β-CD with a similar affinity (unpublished results).

Regarding the inclusion of CDs in the nanocarriers, this has been studied in detail by our laboratory [12,14]. Uncharged CDs show very inefficient inclusion in CS NP matrices. As a matter of fact, we have calculated that for most neutral CDs, only 1–6% of the molecules are included in the nanocarrier. For anionic CDs, inclusion in the NP matrix is very efficient, as it is clearly illustrated by SBE_{7m}-β-CD. Indeed, typically more than 50% of the SBE_{7m}-β-CD is integrated into the NP core [12]. In this work, we have confirmed SBE_{7m}-β-CD inclusion values by analyzing the amount of non-incorporated CD in the NP supernatant through a colorimetric method. The fading of phenolphthalein solutions confirmed that 95% of the SBE_{7m}-β-CD molecules are incorporated to unloaded CS/SBE_{7m}-β-CD NPs, while 79% of the SBE_{7m}-β-CD molecules are incorporated to GSH-loaded CS/SBE_{7m}-β-CD NPs.

In summary, our current understanding of the loading process indicates that CD affinity for the CS NP matrix is the main cause for the EE difference between α-CD and SBE_{7m}-β-CD-containing NPs. However, moderate CD inclusion constants might be the main bottleneck limiting further increases in GSH encapsulation in CS/SBE_{7m}-β-CD NPs. In any case, GSH is an illustrative example of how optimized CS/CD NP formulations can extend the pharmaceutical applicability of standard CS nanoparticles.

3.2. XPS analysis

X-ray Photoelectron Spectroscopy (XPS) is a surface-sensitive technique providing information about the elemental composition of a 5–10 nm thick surface layer. XPS can be operated under several conditions, including conventional, angle-resolved, mapping and depth profiling (ion etch assisted) modes. To date, few works have

reported on the application of this spectroscopic technique to NPs characterization. A recent work is the one of Kommareddy and Amiji [25], where poly(ethylene glycol)-modified thiolated gelatin NPs were characterized by XPS operating in conventional mode. Herein, XPS was performed in the so-called "depth profiling" mode to provide an insight on the in-depth distribution of different target species in CS/SBE_{7m}-β-CD NPs. This specific NP system was selected for XPS analysis because in this system nitrogen, sulphonate and thiol groups can act as unequivocal markers of the presence of CS, SBE_{7m}-β-CD and GSH, respectively. Furthermore, CS/CD NPs prepared from anionic CDs have been recently developed [12,15,16]; and, thus, further characterization is required.

Typical spectra of the pristine and etched NPs are reported in Fig. 2. The S_{2p} region of the pristine material (ion etching time = 0 s) is composed by only one doublet (Binding Energy, $BE_{S2p3/2}$ = 167.6 ± 0.2 eV), attributed to the sulphonate chemical environment of SBE_{7m}-β-CD. As ion-etching exposed inner parts of the nanoparticle, progressively, a second chemical environment became evident in the S_{2p} region. This feature, falling at low binding energy values ($BE_{S2p3/2}$ = 163.4 ± 0.2 eV), was attributed to S–H and S–S groups, belonging to GSH and/or its dimeric species. Therefore, this feature can be used as a marker of the presence of the peptide [26]. Noteworthy, the sulphur atomic percentage slightly increased upon etching (Table 2), and the relative abundance of the sulpho and sulphide species changed during the in-depth analysis (Table 3). In particular, the concentration of the –SH group increased when inner layers were exposed (Fig. 2). Indeed, the concentration of the –SH groups was maximal at 480 s of etching time, which is calculated to approximately correspond with the nanoparticle center. In conclusion, XPS spectroscopy evidences that GSH is more abundant in the inner layers of the NPs, while CS and SBE_{7m}-β-CD are approximately homogenously distributed in the NPs. This different distribution of GSH and SBE_{7m}-β-CD might result surprising at first glance, as the drug is supposed to be loaded into the nanoparticles as complex with the CD. Our interpretation is that GSH encapsulated in the outer layers of the NPs, either alone or as a complex, might diffuse out during the ionic crosslinking process. On the other hand, GSH entrapped in the core of the nanoparticles might remain tightly bound to the nanostructure.

3.3. In vitro release study

In vitro release tests of NPs were carried out in simulated gastric and intestinal media without enzymes (USP XXVI), and very different behaviours were observed for CS, CS/α-CD and CS/SBE_{7m}-β-CD NPs (Fig. 3A and B). Mainly, for CS/SBE_{7m}-β-CD NPs, no detectable amount of GSH release could be observed in any of the tested media. Although this outcome was surprising, as stated before, XPS spectroscopy confirmed that GSH is mainly located in the core of these NPs. Therefore, it can be conceived that GSH diffusion out of NP system might be severely impaired. On the other hand, high percentages of released GSH were observed for CS NPs and

Table 2
Depth-profile XPS elemental analysis of GSH-loaded CS/SBE_{7m}-β-CD NPs subjected to controlled ion erosion. Etch rate was approximately 10 nm/min; therefore, a 480 s etching time corresponds to an etched thickness of about 80 nm, i.e. allows the analysis of the NP core.

Etch time (s)	%C	%O	%N	%S	%Cl
0	68.9	25.0	2.8	2.4	0.9
80	65.9	27.2	3.8	2.4	0.7
160	67.2	25.1	4.0	3.0	0.7
320	71.1	21.3	3.8	3.2	0.6
480	74.7	17.3	4.0	3.4	0.6

Table 3
Abundance (expressed as atomic percentage) of chemical environments of the sulphur atom detected at different etching times.

Etch time (s)	$\%SO_3^-$	%SH
0	2.4	–
80	2.1	0.3
160	2.0	1.0
320	1.8	1.4
480	1.7	1.7

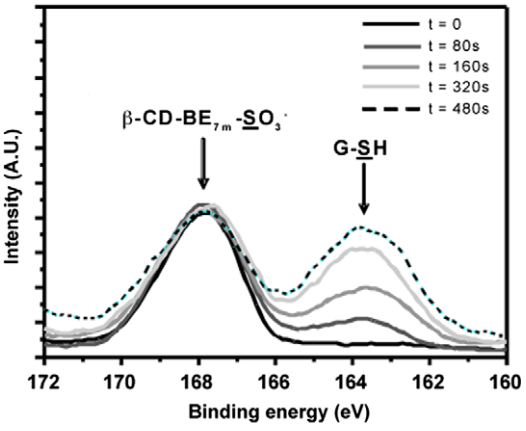

Fig. 2. XPS S_{2p} high-resolution spectra of CS/SBE_{7m}-β-CD NPs obtained at different etching times. (For interpretation of the references to color in this figure legend, the reader is referred to the web version of this paper.)

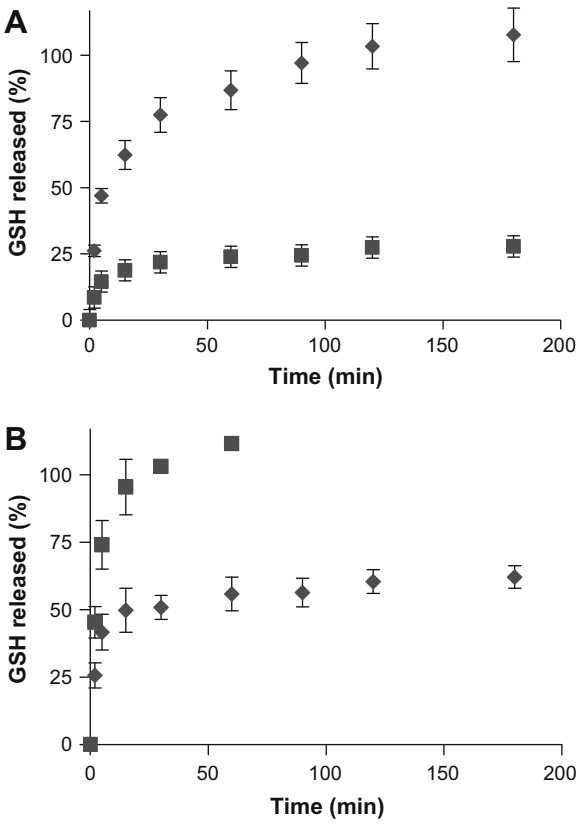

Fig. 3. In vitro release profiles of GSH from (A) CS or CS/CD NPs at pH 1.2 and (B) pH 6.8. Series are: CS NPs (♦); CS/α-CD NPs (■). For CS/SBE_{7m}-β-CD NPs, GSH was below the level of detection for all time points, n = 3.

Table 4
Permeability of GSH trough frog intestine: in solution, in solution and added to blank CS NPs, or in solution and added to blank CS/SBE_{7m}-β-CD NPs. Studies were performed both in the proximal and in the distal segment of frog intestine. Data are mean ± SD, $n = 6$.

	P (cm/s 10^{-6}) GSH alone	P (cm/s 10^{-6}) GSH + CS NPs	P (cm/s 10^{-6}) GSH + CS/SBE_7-β-CD NPs
Proximal segment	3.65 (± 0.57)	5.18 (± 0.22)*	4.86 (± 0.75)**
Distal segment	2.79 (± 0.75)	3.57 (± 0.85)	5.10 (± 0.35)*

* $p < 0.01$ versus GSH alone.
** $p < 0.05$ versus GSH alone.

CS/α-CD NPs (Fig. 3A and B). Such release profiles were similar to those observed with other CS and CS/CD NPs for proteins and low molecular weight drugs [14,24]. The typical fast release profiles observed for CS-based NPs are attributed to a mechanism combining CS/drug complexation equilibrium and diffusion of the drug through the thin CS layer [24,27].

Despite some similarities, CS NPs and CS/α-CD NPs showed several relevant differences regarding their release profiles. In gastric medium, CS NPs released 100% of the loaded GSH over 3 h, whereas CS/α-CD NPs reached a plateau corresponding to approximately 30% of the loaded GSH (Fig. 3A). In intestinal medium, these trends were inverted: CS/α-CD NPs reached 100% release in less than 1 h, whereas CS NPs were only able to release 50% of the loaded GSH in 3 h (Fig. 3B).

In principle, the release profile of CS/α-CD NPs seems to be more suitable for oral GSH delivery as it would protect the drug from the gastric environment and release it once in the intestine. However, release conditions are expected to change dramatically *in vivo*, for instance as a result of the enzymatic degradation of CS. Under such conditions, GSH release process could be triggered from CS/SBE_{7m}-β-CD NPs.

3.4. Transport studies in frog intestine

Finally, we aimed at characterizing the capacity of our nanocarriers to promote GSH transport through physiological epithelia. To study this process, we performed transport experiments in the frog intestine model, which has been established as a reliable *ex vivo* method for predicting peroral drug absorption in humans [28,29]. Furthermore, the intestinal transport of GSH occurs both by passive diffusion and by Na-dependent active transporters (PEPT) [29] and both mechanisms have been described in humans and frogs.

Although administration of GSH encapsulated in CS or CS/CD NPs would have been the most direct test for predicting GSH absorption from our nanocarriers, this study was unfeasible. Firstly, the major limiting factor was the inherent difficulty to extract GSH from the CS NPs, a necessary step prior to its quantification in the donor or acceptor chambers. Furthermore, the detection of the amount of GSH permeated from NPs across frog intestine barrier would have been impossible via HPLC analysis. Thus, we designed a simplified study in which the permeability of GSH in solution is determined, either in the presence or in the absence of blank nanocarriers, in a way that mimics the absorption process of the fraction of GSH that might be released in the intestine under *in vivo* conditions. Concretely, three different systems were studied: (i) GSH in solution, (ii) GSH in solution added to blank CS NPs and (iii) GSH in solution added to blank CS/SBE_{7m}-β-CD NPs. Furthermore, to better illustrate the behaviour of our pharmaceutical systems, we have separately considered two segments of the frog intestine (i.e. the proximal and the distal segment), where different transporters might be expressed. We have also taken into account the inter-season variability of frog intestine, which is known to cause different expression of transporters. For this reason, the experiments were performed according to a scheduled calendar.

The absorption of GSH (alone or dispersed with the tested blank particles) presented a lag time of 30 min prior to any HPLC signal could be detected. GSH transport over time was estimated by curve fitting with a linear model as described in the Methods section, and the permeability coefficients were calculated. Permeability coefficients of GSH are shown in Table 4. As it can be seen, the permeability coefficients of GSH in the intestine were moderate (Table 4). In the proximal segment of duodenum, both NP formulations were able to provide statistically significant improvements of the permeability coefficient of GSH, with values that were 1.4 times bigger than the control. Interestingly, in the distal segment of the intestine, only CS/SBE_{7m}-β-CD NPs were able to provide significant enhancements in GSH transport. Indeed, in this segment, the permeability coefficient of GSH in solution added to blank CS/SBE_{7m}-β-CD NPs was almost twice than that of control (Table 4). Although we cannot provide solid explanations concerning the different behaviour of CS and CS/SBE_{7m}-β-CD NPs in the different regions of the intestine at this stage, it is important to note that the gut is asymmetric regarding morphology, thickness of the epithelium and expression of transporters [30]. Therefore, the intrinsic physicochemical properties of CS/SBE_{7m}-β-CD NPs (i.e. smaller size, potential chelating capacity of SBE_{7m}-β-CD) might result in different interactions of the particles with the surrounding epithelium.

4. Conclusions

In this study, nanoparticles consisting of chitosan and selected cyclodextrins have been prepared and characterized *in vitro* as potential formulations for oral GSH delivery. Our studies confirm that by selecting the most suitable cyclodextrin, we can modulate the physicochemical characteristics of the nanoparticles and their ability to load GSH. Chitosan nanoparticles containing the anionic cyclodextrin SBE_{7m}-β-CD seem to be highly interesting as potential oral GSH carriers, as they combine improved GSH loading with the capacity to promote GSH transport through the intestine, as observed in a frog intestinal sac model.

Acknowledgements

This project was financed by Università degli Studi di Bari (Progetti d'Ateneo). We thank Ramiro Barreiro Perez (Unidad de Microscopia Electronica, Universidad de Santiago de Compostela, Spain) for his valuable help with TEM studies. MGF is a recipient of an Isidro Parga Pondal Contract (Xunta de Galicia, Spain).

References

[1] S.S. Langie, A.M. Knaapen, J.M.J. Houben, F.C. van Kempen, J.P.J. de Hoon, R.W.H. Gottschalk, R.W.L. Godschalk, F.J. van Schooten, The role of glutathione in the regulation of the nucleotide excision repair during oxidative stress, Toxicol. Lett. 168 (2007) 302–309.
[2] Martindale, The Complete Drug Reference, 33th ed., The Pharmaceutical Press, London, Great Britain, 2002, pp. 1010–1011.
[3] H. Demopoulos, M.L. Seligman, PCT Int WO98/29101.

[4] E. Camera, M. Picardo, Analytical methods to investigate glutathione and related compounds in biological and pathological processes, J. Chromatogr. B 781 (2002) 181–206.
[5] M. Tobio, A. Sanchez, A. Vila, C. Soriano, J.L. Evora, J.L. Vila-Jato, M.J. Alonso, Investigations on the role of PEG on the stability in digestive fluids and in vivo fate of PEG–PLA nanoparticle following oral administration, Colloids Surf. B: Biointerf. 18 (2000) 315–32330.
[6] G. Sandri, M.C. Bonferoni, S. Rossi, F. Ferrari, S. Gibin, Y. Zambito, G. Di Colo, C. Caramella, Nanoparticles based on N-trimethylchitosan: evaluation of absorption properties using in vitro (Caco-2 cells) and ex vivo (excised rat jejunum) models, Eur. J. Pharm. Biopharm. 65 (2007) 68–77.
[7] Y.-H. Lin, F.-L. Min, C.-T. Chen, W.-C. Chang, S.-F. Peng, H.-F. Liang, H.-W. Sung, Preparation and characterization of nanoparticles shelled with chitosan for oral insulin delivery, Biomacromolecules 8 (2007) 146–152.
[8] R. Fernandez-Urrusuno, D. Romani, P. Calvo, J.L. Vila-J, M.J. Alonso, Development of freeze-dried formulation of insulin loaded chitosan nanoparticles intended for nasal administration, STP Pharma Sci. 9 (5) (1999) 429–436.
[9] Y. Pan, Y. Li, H. Zhao, J. Zheng, H. Xu, G. Wei, et al., Bioadhesive polysaccharide in protein delivery system: chitosan nanoparticles improve the intestinal absorption of insulin in vivo, Int. J. Pharm. 249 (2002) 139–147.
[10] Y. Zhang, Y. Yang, K. Tang, X. Hu, G. Zou, Physicochemical characterization and antioxidant activity of quercetin-loaded chitosan nanoparticles, J. Appl. Polym. Sci. 107 (2008) 891–897.
[11] N. Csaba, M. Garcia-Fuentes, M.J. Alonso, The performance of nanocarriers for transmucosal drug delivery, Expert. Opin. 3 (4) (2006) 463–478.
[12] A. Trapani, M. Garcia-Fuentes, M.J. Alonso, Novel drug nanocarriers combining hydrophilic cyclodextrins and chitosan, Nanotechnology 19 (18) (2008) 185101/1–185101/10.
[13] A.H. Krauland, M.J. Alonso, Chitosan/cyclodextrin nanoparticles as macromolecular drug delivery system, Int. J. Pharm. 340 (2007) 134–142.
[14] F. Maestrelli, M. Garcia-Fuentes, P. Mura, M.J. Alonso, A new drug nanocarrier system consisting of chitosan and hydroxypropylcyclodextrin, Eur. J. Pharm. Biopharm. 63 (2) (2006) 79–86.
[15] D. Teijeiro-Osorio, C. Remuñan-Lopez, M.J. Alonso, Chitosan/cyclodextrin nanoparticles can efficiently transfect the airway epithelium in vitro, Eur. J. Pharm. Biopharm. 71 (2009) 257–263.
[16] D. Teijeiro-Osorio, C. Remuñan-Lopez, M.J. Alonso, New generation of hybrid poly/oligosaccharide nanoparticles as carriers for the nasal delivery of macromolecules, Biomacromolecules 10 (2) (2009) 243–249.
[17] M. Garcia-Fuentes, A. Trapani, M.J. Alonso, Protection of the peptide glutathione by complex formation with α-cyclodextrin: NMR spectroscopic analysis and stability study, Eur. J. Pharm. Biopharm. 64 (2006) 146–153.
[18] P. Calvo, C. Remuñan-Lopez, J.L. Vila-J, M.J. Alonso, Novel hydrophilic chitosan–polyethylene oxide nanoparticles as protein carriers, J. Appl. Polym. Sci. 63 (1997) 125–132.
[19] E. Ieva, A. Trapani, N. Cioffi, N. Ditaranto, A. Monopoli, L. Sabbatini, Analytical characterization of chitosan nanoparticles for peptide drug delivery applications, Anal. Bioanal. Chem. 393 (2009) 207–215.
[20] A.M. Da Silveira, G. Ponchel, F. Puisieux, D. Duchene, Combined poly(isobutylcyanoacrilate) and cyclodextrins nanoparticles for enhancing the encapsulation of lipophilic drugs, Pharm. Res. 15 (1998) 1051–1055.
[21] A. Lopedota, A. Trapani, A. Cutrignelli, L. Chiarantini, E. Pantucci, R. Curci, E. Manuali, G. Trapani, The use of Eudragit RS 100/cyclodextrin nanoparticles for the transmucosal administration of glutathione, Eur. J. Pharm. Biopharm. 72 (2009) 509–520.
[22] Z. Ma, T.M. Lim, L.-Y. Lim, Pharmacological activity of peroral chitosan–insulin nanoparticles in diabetic rats, Int. J. Pharm. 293 (2005) 271–280.
[23] K.A. Janes, P. Calvo, M.J. Alonso, Polysaccharide colloidal nanoparticles as delivery systems for macromolecules, Adv. Drug Deliv. Rev. 47 (2001) 83–97.
[24] Y. Aktas, K. Andrieux, M.J. Alonso, P. Calvo, R.N. Gursoy, P. Couvreur, Y. Capan, Preparation and in vitro evaluation of chitosan nanoparticles containing a caspase inhibitor, Int. J. Pharm. 298 (2005) 378–383.
[25] S. Kommareddy, M. Amiji, Poly(ethylene glycol)-modified thiolated gelatine nanoparticles for glutathione-responsive intracellular DNA delivery, Nanomedicine 3 (2007) 32–42.
[26] K.J. Cantrell, S.B. Yabusaki, M.H. Engelhard, A.V. Mitroshkov, E.C. Thornton, Oxidation of H_2S by iron oxides in unsaturated conditions, Environ. Sci. Technol. 37 (2003) 2192–2199.
[27] M. Hamidi, A. Azadi, P. Rafiei, Hydrogel nanoparticles in drug delivery, Adv. Drug Deliv. Rev. 60 (2008) 1638–1649.
[28] M. Franco, A. Lopedota, A. Trapani, A. Cutrignelli, D. Meleleo, S. Micelli, G. Trapani, Frog intestinal sac as an in vitro method for the assessment of intestinal permeability in humans: application to carrier transported drugs, Int. J. Pharm. 352 (2008) 182–188.
[29] G. Trapani, M. Franco, A. Trapani, A. Lopedota, A. Latrofa, E. Gallucci, S. Micelli, G. Liso, Frog intestinal sac: a new in vitro method for the assessment of intestinal permeability, J. Pharm. Sci. 93 (2004) 2909–2919.
[30] T.Z. Csaky, E. Gallucci, Seasonal variation in the active transporting ability and in the membrane ATPase activity of the frog intestinal epithelium, Biochim. Biophys. Acta 466 (1977) 521–525.